

# INVESTIGATION OF MICROSTRUCTURAL AND MECHANICAL PROPERTIES OF 7075 AL ALLOY PREPARED BY SIMA METHOD

H. Mohammadi\* and M. Ketabchi

\* h.mohammadi63@gmail.com

Received: March 2013

Accepted: July 2013

Department of Mining and Metallurgical Engineering, Amirkabir University of Technology, Tehran, Iran.

**Abstract:** The microstructure and mechanical properties of 7075 wrought aluminum alloy produced by strain induced melt activation (SIMA) route were investigated. Also liquid volume fraction measurement was studied by three procedures. Remelting process was carried out in the range of 560 to 610 °C for 20 min holding. The microstructure in the semi-solid state consists of fine spherical solid grains surrounded by liquid. The mechanical properties of the alloy vary with the grain size and weak mechanical properties of globular samples would appear if an alloy reheated at a high temperature. Thermodynamic simulation is a fast and efficient tool for the selection of alloys suitable for semi-solid processing.

**Keywords:** 7075 Al alloy; Semi-solid microstructure; Mechanical property

## 1. INTRODUCTION

Semi-Solid Forming (SSF) is a novel technology in forming near net shape components in the 21st century, offering several potential advantages over conventional casting and forging technologies such as high product quality and low forming efforts [1-3]. The key to SSF is fabricating the semi-solid materials with a globular microstructure [2]. Many methods such as mechanical or electromagnetic stirring, the addition of grain refining elements, and cooling slope are used to obtain globular structures [2-3]. Among the production methods, SIMA is an ideal candidate with significant commercial advantages of simplicity and low equipment costs. In this route, the material is deformed by extrusion or other processes and then reheated to semisolid state which recrystallization occurs and liquid metal penetrates in the recrystallized grain boundaries thus resulting in solid globular particles surrounded by liquid [4-7]. Parameters such as heating time, temperature and the degree of cold working are critical factors in controlling the semi-solid microstructures in the SIMA process [6].

Some studies on the microstructure evolution of semisolid slurry of AA5013 aluminum alloy [8], 2024 aluminum alloy [9-10] and AZ91D magnesium alloy [7,11, 12] have been carried out. However, little was reported on the

microstructure and mechanical evolution of 7075 Al alloy semisolid slurry prepared by SIMA. The purpose of the present work is to evaluate the effect of holding temperature on the microstructure and mechanical properties of a semisolid 7075 Al alloy during reheating process.

## 2. EXPERIMENTAL PROCEDURES

The material used in this study was 7075 Al alloy rod with an extrusion ratio of 20. Chemical composition of the studied alloy is listed in Table 1.

The dependency of liquid fraction on temperature and differential thermal analysis (DTA) experiment were carried out with a constant heating rate of 0.2 °C/s. Cubic specimens of 10×10×10 mm were used in this experiment to investigate the microstructure. The main objective of the experiments was the evaluation of influence of SIMA process parameters (isothermal temperature and time) on the resulting microstructure and mechanical properties. In order to study the effect of isothermal temperature on the semisolid microstructure, the predeformed samples were

**Table 1.** Composition of aluminum alloy used in this study (wt %).

| Zn  | Mg  | Cu  | Fe   | Si  | Cr   | Mn   | Ti   | Al  |
|-----|-----|-----|------|-----|------|------|------|-----|
| 5.6 | 2.4 | 1.4 | 0.42 | 0.4 | 0.26 | 0.13 | 0.01 | Bal |

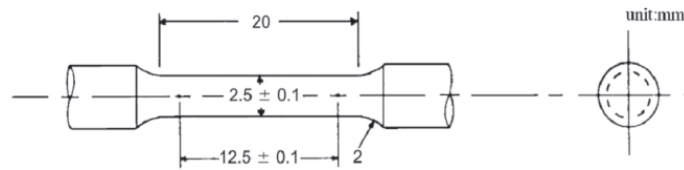


Fig.1. Schematic for tensile specimen

reheated in the electric resistance furnace at the temperatures of 560, 570, 580, 590, 600 and 610°C for 20 min. The holding time was measured from the moment that the furnace reached the respective temperature. And to investigate the effect of time, the predeformed samples were held at 580 °C for 10, 20 and 30 min, respectively. After the heat treatment, the samples were quenched in water at room temperature to keep the microstructure morphology of semisolid in the room temperature. Samples for microstructure characterization were prepared by the standard metallurgical technique, followed by etching in a keller's reagent (mixed acid solution of HF, HCl and HNO<sub>3</sub>). The microstructure of the samples was observed under metallographic microscope. Quantitative metallographic analysis including the liquid volume fraction, average grain size and shape factor of solid phase were performed using an image analyzing system (Clemex Software). The line scan was conducted by wavelength dispersive X-ray (WDX) analytical system in the scanning electron microscope (SEM). To study the effect of isothermal temperature on the mechanical properties, the macro-hardness examination was performed on an Optical Brinell–Rockwell–Vickers hardness tester, by imposing a load of 10 kg for 10 second. Averages of five values were examined in different locations of each small specimen were taken as the hardness of each small specimen. And the average of hardness of the three small specimens was taken as the hardness of a product.

The tensile tests were performed to evaluate and compare the strength and ductility of reheated samples with as-received samples. The specimens firstly were diced from initial as-received material to the rectangular shape samples with the 10×10×40 mm and reheated to semisolid range, then were quenched and

machined to required shape for tensile test as shown in Fig.1 [13]. Tensile tests were performed at room temperature using a Zwick universal testing machine. Tensile curves were analyzed to determine the ultimate tensile strength (UTS) and elongation to failure. The resulting UTS and elongation were the average of three bars. The fracture surfaces of the tested tensile specimens were examined using a SEM.

### 3. EXPERIMENTAL RESULTS AND DISCUSSION

#### 3. 1. Effects of Isothermal Temperature and Time on the Microstructure

The initial as-received microstructure of the extruded billet is shown in Fig. 2. Microstructures is very similar to hot worked metals with unrecrystallized and elongated grains and intermetallic particles aligned in the extrusion direction.

The microstructure evolution during the SIMA process can be divided into four stages including: (1) deformation, (2) recovery and recrystallization, (3) partial remelting, and (4) spheroidizing and grains coarsening. The deformation ratio, produce a great influence on both the second and third stage [12]. During the plastic deformation of the specimens, internal strain energy is stored in forms of dislocation multiplication, elasticity stress, and vacancies, which provides the driving force for recovery and recrystallization. The energy increases with the plastic deformation ratio, which boost the morphological change from dendritic and unequiaxed to globular structure, in other words globularization occurs faster and globularity of solid grains will be higher. When the alloy have been heated just above the solidus, grain boundaries were gradually penetrated by liquid due to the dissolution of the last solidified phase

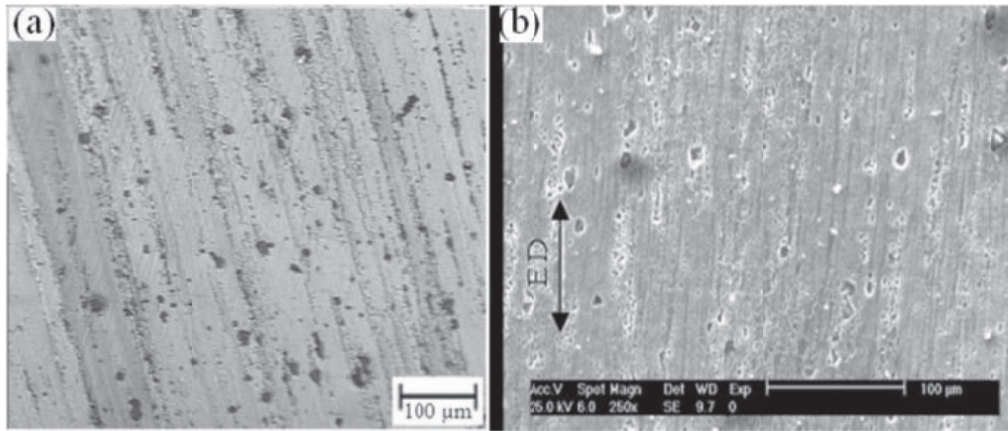


Fig. 2. The optical (a) and SEM (b) microstructure of as-received specimen with an extrusion ratio of 20.

of low melting temperature. As soon as liquid phase has occurred at grain boundaries, grain spheroidization and coarsening were activated simultaneously [12].

Fig. 3 shows the quenched microstructures after isothermal treatment at different temperatures of 560, 570, 580, 590, 600 and 610°C for 20 min. The microstructures consist of  $\alpha$ -Al solid grains, liquid phase, and the entrapped liquid droplets inside the solid grains. And it could be observed that with increasing isothermal temperature, the liquid phase increased, the thickness of grain boundary liquid film was thicker, the grains size grow larger and the shape of the solid grains became more globular. The

two main mechanisms of grain coarsening play an important role during partial remelting. One of the coarsening mechanisms is the coalescence of grains. Grain growth by coalescence by grain boundary migration is dominant at short times after liquid is formed and at low volume fractions of liquid. Liquid fraction increases with an increase of the temperature and holding time. Because of the liquid phase soakage, it is difficult for the adjoining grains to coalesce continuously. Under these conditions, Ostwald ripening is the dominating mechanism of grain coarsening in the stage of high liquid fraction, in which grains continuously coarsen and the small grains gradually melt [10-11]. Ostwald ripening

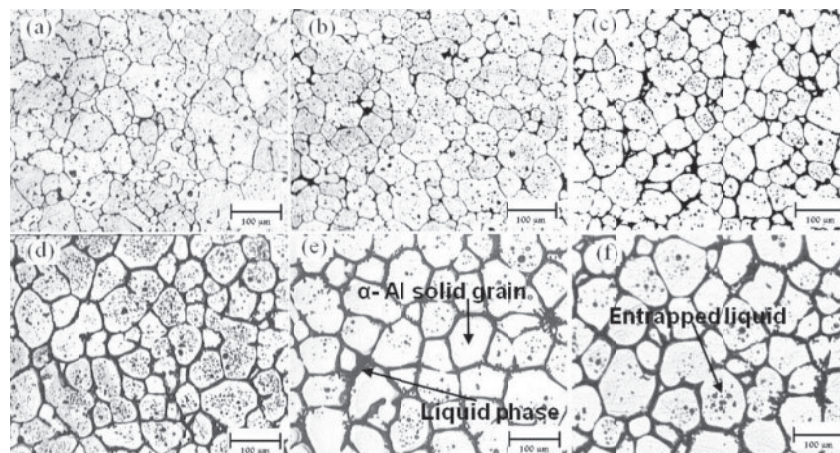


Fig. 3. Effect of heating temperature on microstructure for 20 min: (a) 560, (b) 570, (c) 580, (d) 590, (e) 600 and (f) 610 °C.

and grain coalescence operate simultaneously and independently as soon as liquid is formed. Grain coalescence in the alloy is controlled by solid-solid contacts and grain contacts lead to an increase in grain growth rate and especially the irregular shape (Fig. 3 (d)). Average grain size ( $d$ ) and shape factor ( $SF$ ) of solid phase were measured from microstructures using an image analysis system. Size and globularity of solid grains were calculated in each case by applying the Eqs. (1) and (2) [14].

$$d = \frac{\sum_{N=1}^N \sqrt{4A / \pi}}{N} \quad (1)$$

$$SF = \frac{\sum_{N=1}^N \frac{4\pi A}{P^2}}{N} \quad (2)$$

In these equations,  $A$ ,  $N$  and  $P$  are area, the number and perimeter of solid grains, respectively.  $SF$  is a value closing to 1, corresponding to better globularity of solid grains. Fig. 4 shows the effect of isothermal temperature on the average grain size and of the solid grains. Solid grain size measurement shows a continuous increase of the solid grain size as the isothermal temperature increased. The quantitative microstructure examination indicates

that the average solid grain size decreases while reheating from 560 to 570°C and then increases. With the increasing of temperature, ripening mechanism does an effect on the average size of the solid grains, which increases it. Also because of the effect of interface curvature, the solid grains easily become globular.

$SF$  measurement shows that the solid grain tended to become more spherical with increasing temperature from 560 to 610 °C. The  $SF$ , is an important parameter for thixoforming, because it has strong influence on the flowability and the viscosity of the material. With increasing temperature, liquid soak aging leads to increasing globularity. In addition, calculated results (Fig.4) indicate clearly that the appropriate and optimum condition can be obtained at reheating temperature of 580 °C, the average grain size was less than 70 μm and  $SF$  was almost closing to 0.7. The effects of holding time on microstructure during partial remelting are shown in Fig. 5. The effects of increasing holding time are similar to the effects of increasing reheating temperature, but have a lesser effects.

It can be seen from Fig.5, the microstructure in the semi-solid state consisted of fine and spherical solid grains, which were uniformly distributed in liquid matrix. There was no significant change in the average grain size by increasing holding time but the microstructure

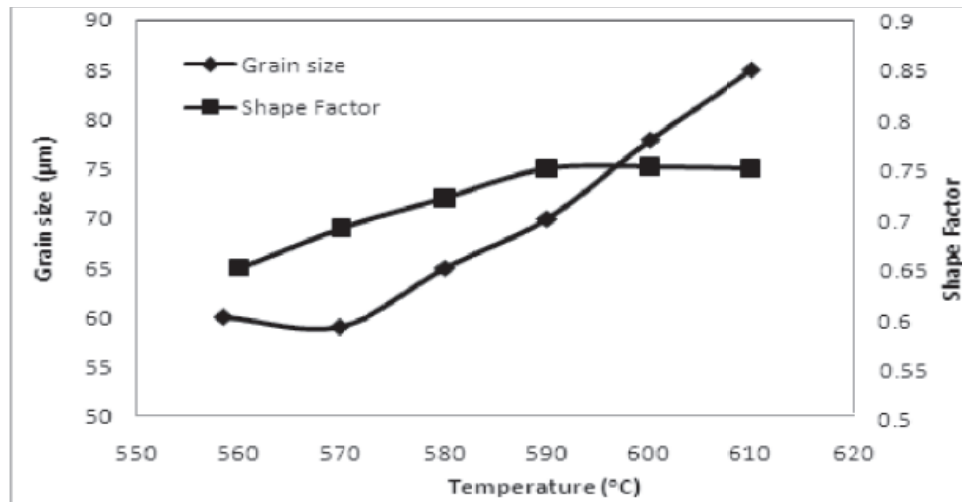


Fig. 4. Effects of temperature on average size and shape factor of the solid grains

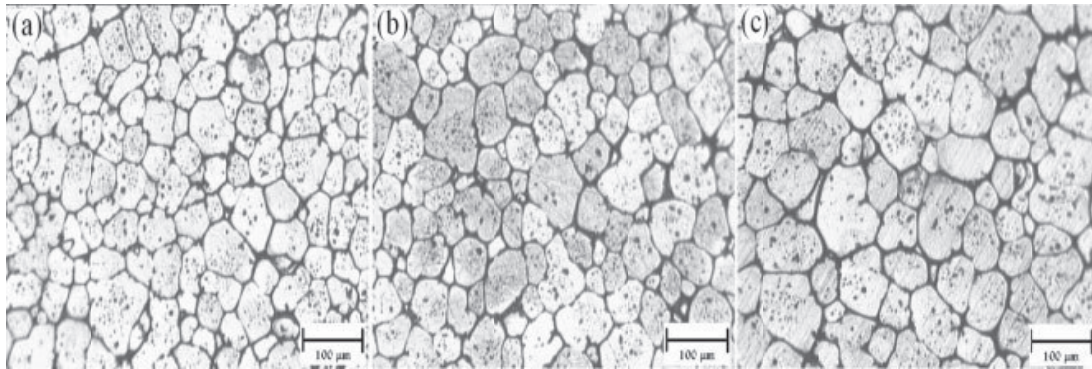


Fig. 5. Effect of holding time on microstructures at 580 °C for: (a) 10, (b) 20 and (c) 30 min

becomes more uniform. Therefore, the samples were reheated at 580°C for less than 30 min, are desirable for thixoforming at high solid fraction.

### 3. 2. Results by DTA and WDX

The DTA curve is shown in Fig. 6. Through the extrapolation of starting and ending of reaction points in Fig. 6, the solidus and liquidus temperatures were determined to be 470 °C and

635 °C, respectively. Backerud et al. have carried out research into the solidification reactions based on thermal analysis, metallography, and energy dispersive X-ray spectroscopy analysis [15]. Table 2 shows the reactions that occur in the 7075 system when fully liquid melt is cooled through the solidification range [15].

Whereas, the melting sequence (from Fig. 6) matches the solidification sequence (from Table 2), the first reaction that turn into a liquid during

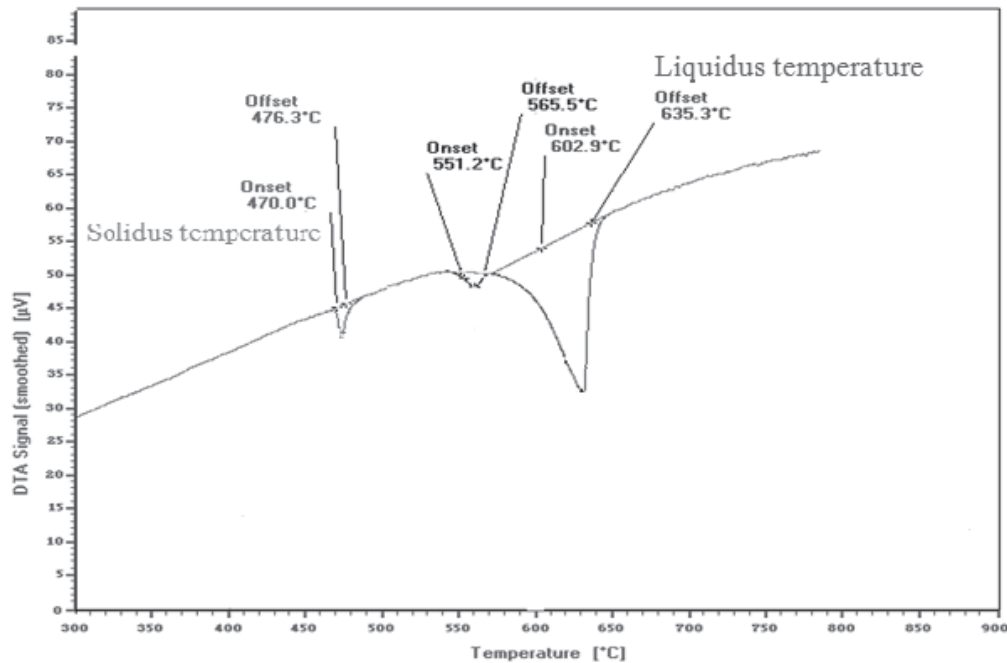


Fig. 6. DTA curveduring heating of the 7075 alloy

**Table 2.** The reactions take place when 7075 Al alloy is cooled through the solidification range with 0.3 cooling rate (K/s) [15]

| Reaction sequence | Reaction type  | Reaction temperature |
|-------------------|--|----------------------|
| First reaction    | Liquid → Al, dendritic network                       | 630-623°C            |
| Second reaction   | Liquid → Al + Al <sub>3</sub> Fe                     | 618-615°C            |
| Third reaction    | Liquid → Al + Mg <sub>2</sub> Si                     | 568-563°C            |
| Fourth reaction   | Liquid → Al + Al <sub>2</sub> Cu + MgZn <sub>2</sub> | 469°C                |

reheating would be the MgZn<sub>2</sub> and Al<sub>2</sub>Cu at around 470 °C (solidus temperature) as shown in Fig.6. The reaction between Al and Mg<sub>2</sub>Si at around 551°C is the next reaction that will result in formation of liquid.

Inside the alloy in semisolid state, the microstructure is composed of solid phase grains with high melting point, which surrounded by melting liquid phase and there exist large differences in the element content and phase composition between the solid phase and liquid

phase. The eutectic phase at the grain boundary remelted firstly because these are generally areas with higher solute concentrations and formed small amount of liquid phase. The condition for grain boundary wetting is satisfied when:  $2\gamma_{SL} \leq \gamma_{SS}$ , where  $\gamma_{SL}$  is the solid/liquid interfacial energy and  $\gamma_{SS}$  is the energy of the solid grain boundary [15]. Other words, grain boundaries with higher distortion energy melt faster during reheating. As soon as liquid is present at these boundaries the grains begun to grow, so spheroids surrounded by

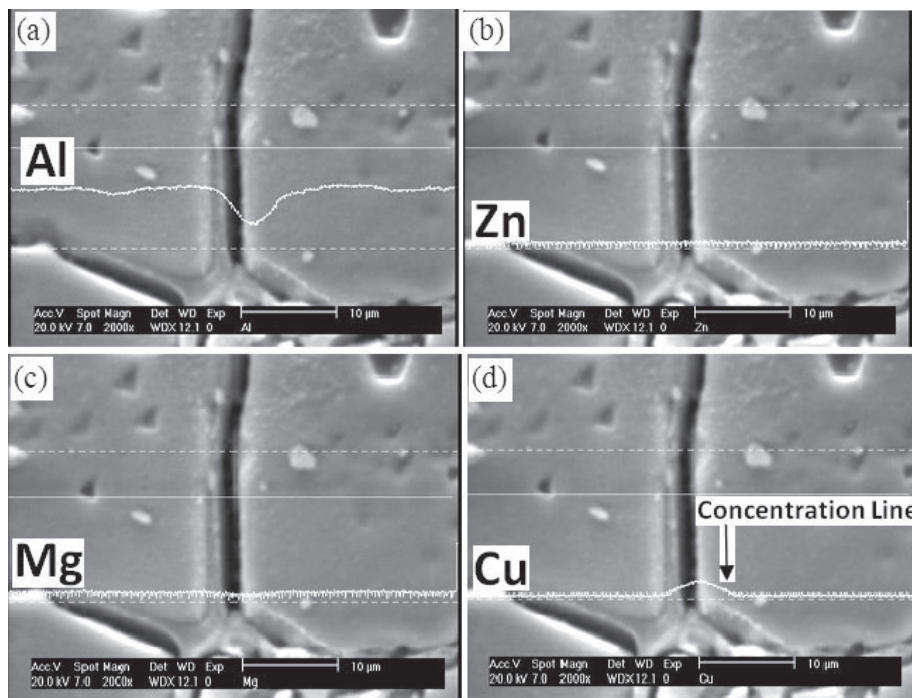


**Fig. 7.** Results of line scan by WDX of specimen held at 580 °C for 20 min: (a) Al line scan; (b) Zn line scan (c) Cu line scan; (d) Mg line scan

liquid. Then the periphery of solid grains remelted partially through the solute diffusion at the solid/liquid interface. As a result, the liquid fraction increases continuously.

Fig.7 shows the distribution of the major elements at the semisolid state by line scan analysis. The peak intensity of an element shows the average concentration of the element between the horizontal lines. It can be seen that the Al content concentration in the liquid phase (grain boundary) is lower than in the spherical solid phase (Fig.7 (a)), but the Cu concentration is high in the liquid phase (grain boundary) (Fig.7 (c)). From the Fig.7 (b) and (d), it is seen that the Mg and Zn concentration have not obviously change. In this process, the material melts locally at the grain boundaries due to the marginally enriched

alloying elements there and the associated lower solidus temperature. Content of Cu at grain boundary increased, this means that the low melting structure at grain boundary was much influenced by Cu.

### 3. 3. MECHANICAL PROPERTIES

The mechanical properties of thixoformed 7075 aluminum alloy component strongly depend on the mechanical properties of 7075 Al alloy before thixoforming. The higher mechanical properties of 7075 Al alloy after reheating at semisolid range, lead to the higher mechanical properties of thixoformed components. Fig. 8(a) shows the variations of macro-hardness ( $H_v$ ), as a function of temperature

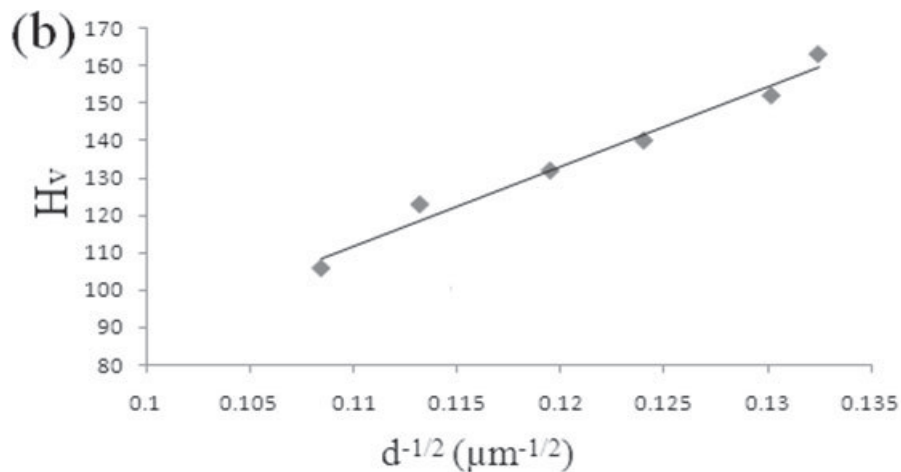


Fig. 8. Macro-hardness of the reheated sample as a function of (a) semisolid temperature and (b) grain size based on  $H_v$  (Vickers) data

in the semisolid range. The  $H_V$  value continues to decrease with increasing temperature. This trend is consistent with the grain-size increase with increasing temperature.

Fig. 8(b) shows the relation of  $H_V$  against  $d^{-1/2}$  was plotted using the data in Fig. 8(a) in order to examine the Hall–Petch relationship for the semisolid processed 7075 Al alloy [16]:

$$H_V = H_O + K_H d^{-1/2} \quad (3)$$

Where  $H_O$  and  $K_H$  are the material constants. Most of the datum points lie on a single straight line depicted by Eq.(3). The mechanical properties of the alloy vary with the grain size and the relationship usually follows the well known Hall–Petch equation. The macro-hardness of as-received materials without T6 temper is 190 Vickers. As shown in Fig. 8(b) with decreasing grain size (increasing  $d^{-1/2}$ ), the macro-hardness,  $H_V$  increased. Increasing of the holding temperature led to coarsening of the grains for the same amount of holding time. As a result, weak

mechanical properties of thixoformed product would appear if an alloy reheated at a high temperature. Table 3 shows a comparison of mechanical properties of 7075 alloy specimens processed at different conditions. The UTS and elongation of the as-received samples without T6 heat treatment is about 530 MPa and 9.7, respectively. In addition, Table 3 shows the mechanical properties of 7075 Al alloy as standard conditions under T6 treatment for comparing the different steps of processes in this study.

To study the tensile behavior of the samples with globular microstructure after reheating process, the samples, which are processed at isothermal temperature of 580 °C and holding time of 20 min, were tested. The UTS and elongation are 219 MPa and 5.1, respectively. Tensile behavior of globular microstructure specimens is completely elastic. According to table 3 the mechanical properties of globular microstructure specimens in comparison with as-received materials are quite weak. Because in

**Table 3.** Mechanical properties of samples with globular microstructure, as-received materials without T6 compared with the 7075 T6 standard

| Alloy Condition              | UTS (MPa) | Elongation (%) |
|------------------------------|-----------|----------------|
| 7075-T6                      | 572       | 11             |
| 7075(As-received-without T6) | 530       | 9.7            |
| Globular microstructure      | 220       | 5.1            |

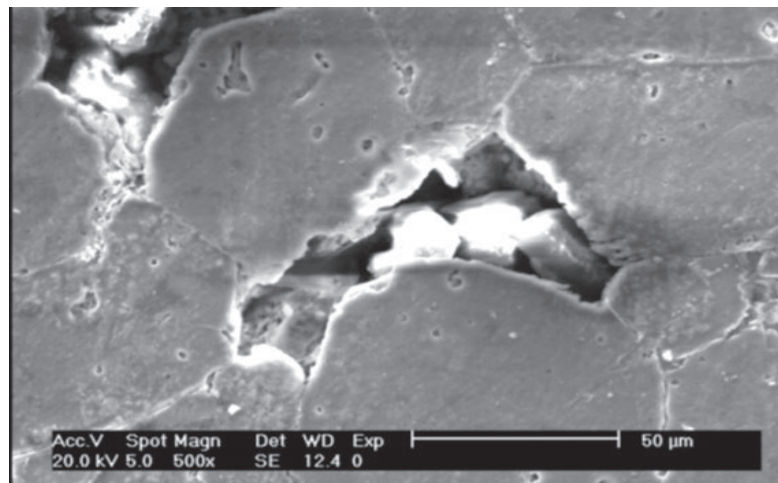


**Fig. 9.** The large porosity among solid globules.



quenched specimens, liquid film among globular solid grains were solidified quickly. Thus, shrinkage porosities, gas porosities and extended porosities were entrapped in the specimens, and are responsible for deterioration of mechanical properties.

The UTS is largely determined by the amount of defects present in the alloy. The major defects affect the ultimate tensile strength (UTS) are gas pores and microstructural non-uniformity. Presence of liquid phase in grain boundaries, results in formation of shrinkage porosities after solidification which reduces tensile properties of specimens.

Fig. 9 shows a large porosity among globular grains. Ultimate strength of globular microstructure specimens has a low value which is due to the presence of shrinkage porosities inside the grains and boundaries. Fig.10 represents the SEM fractographs of the tensile fractured specimens with globular microstructure that reheated at 580 °C with the holding time of 20 min. As can be seen in Fig.10 (a) showed intergranular (typically dimple) fracture mode. Dimples size, depending on the temperature. With attention to presence of liquid film and shrinkage porosities in grain boundaries, the fracture occurred completely intergranular, and the grain deformation rarely took place which resulted brittle fracture and low elongation value for specimens with globular microstructure.

Presence of liquid phase in grain boundaries and inside the globular grains, results in formation of shrinkage porosities after solidification, which reduces elongation of specimens. Higher magnification of fracture surface shown in Fig.10 (b) reveals that globules were detached from sites where liquid film was quenched without undergoing remarkable plastic deformation. Apart from liquid film effects, large porosities represented in Fig.10 (b) decrease the critical fracture stress because of increasing stress concentration and increase susceptibility of the globule boundaries to crack propagation. Thus, due to these defects, intergranular fracture occurred in low level of stress during tension test.

#### 3. 4. Measurement of Liquid Volume Fraction

Liquid fraction controls largely the rheological behavior and the evolution of microstructure in the semisolid state. Thus, this parameter is of critical importance, both for fundamental work and for the control of the industrial process. Therefore, it is important to evaluate the variation of the liquid fraction with temperature. For the determination of the liquid volume fraction, various processes are used, which define the solid phase fraction directly or by means of its effect on special physical properties. Such as thermodynamic data, thermal processes and quantitative metallography by means of quenched

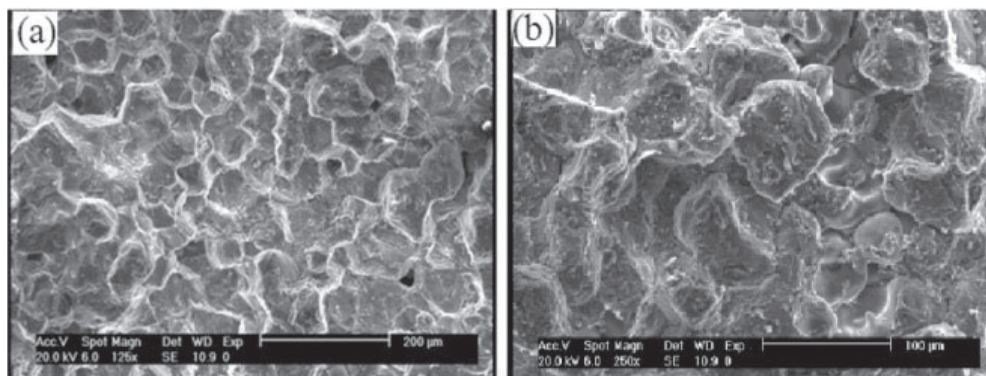


Fig. 10. SEM image of: (a) fracture surface in globular-microstructure specimen, (b) large porosities among globules in globular-microstructure specimen.

samples from the semi-solid range [2]. In practice, these three methods are mostly used. The aim of this section was to investigate quantitatively the effect of the temperature on the liquid fraction evolution during solidification in the Al–Zn–Mg–Cu system. In order to simulate the solidification, in particular the liquid fraction present as a function of temperature and composition, we used the Scheil–Gulliver model for a more realistic description [11]. For Al alloys, this model gives fast and reliable results. The diffusion in the liquid phase is much faster than in the solid phase(s) and it is often a useful approximation to assume that there is no diffusion at all in the solid phase(s) and in finitely fast diffusion in the liquid phase during solidification. This is called Scheil–Gulliver solidification. For simple binary alloys, the non-equilibrium lever rule, or Scheil equation (Eq.(4)), can be used for the analytical determination of the liquid volume fraction,  $f_L^{sch}$ , at a given temperature in the semisolid range [11], which assume that homogenization of the liquid is complete, whit no diffusion in solid :

$$f_L^{sch} = \left( \frac{T_M - T}{T_M - T_L} \right)^{-1/(1-K)} \quad (4)$$

**Table 4.** Required parameters for calculation of liquid volume fraction by Scheil equation.

| $i$ | $c_i$ (Wt%) | $m_i$ | $k_i$ |
|-----|-------------|-------|-------|
| Zn  | 5.6         | 2.12  | 0.53  |
| Mg  | 2.4         | 5.83  | 0.31  |
| Cu  | 1.4         | 3.52  | 0.122 |

Where  $T_M$  the melting temperature of the pure metal is,  $T_L$  is the liquidus temperature of the alloy, and  $k$  is the equilibrium distribution coefficient. Based on DTA and binary phase diagram [17], the values of  $T_L$  and  $T_M$  are 635 °C and 660 °C, respectively.

Assuming that the interactions among various alloying elements are neglected and then  $k$  of multicomponent is obtained using the equivalent pseudo-binary method, which is expressed as [18]:

$$k = \frac{\sum m_i c_i k_i}{\sum m_i c_i} \quad (5)$$

Where  $C_i$  is the initial composition of the  $i$  alloying element,  $m_i$  and  $k_i$  are the liquidus slope

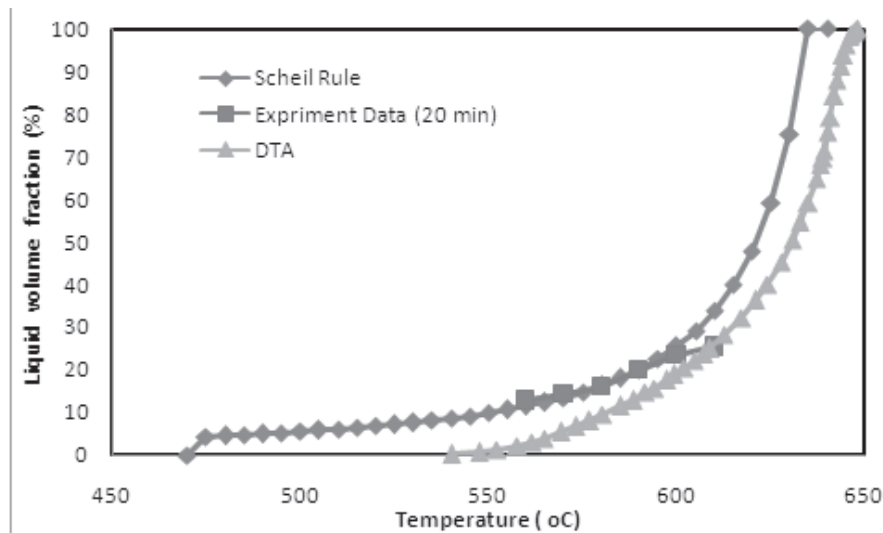


**Fig. 11.** Liquid Fraction vs. temperature given by non-equilibrium (Scheil) equation and DTA analysis compared with metallographically determined liquid-phase contents for 7075 alloy

and partition coefficient of  $i$  element in the  $Al-i$  binary alloys, respectively. Under the experimental condition of this work,  $i$  are Zn, Mg and Cu elements. Elements with very small concentrations (in parentheses) were not considered in the calculations. Based on the binary phase diagram, required parameters for Scheil equation are given in table 4. From table 4 the  $k$  value was calculated and equal 0.362. Therefore, the liquid fraction in the semisolid range obtains from Eqs. (4) and (5).

Fig.11 show the calculations of the liquid fraction/temperature relationship using an analytical solution based on Scheil equation for Al–Zn–Mg–Cu system.

Thermal analysis techniques have been used traditionally in order to evaluate the liquid volume fraction. Using DTA, it is necessary to prepare the alloys in order to be able to have samples. This would involve a long experimentation time to analyze a system like Al–Zn–Mg–Cu.

However, thermodynamic modeling allows the investigation of liquid fraction without the need to prepare any material. Quenching experiments are used to freeze the microstructure in the semisolid state and permit the evaluation of the volume fraction of solid using quantitative metallography. The cooling rate during quenching has to be very fast. Image analysis is used to calculate the solid volume fraction from images of the quenched microstructure, typically obtained by optical microscopy. The area selected for analysis from the quenched sample must be representative for the alloy. Samples must be prepared very carefully. Bad image quality from preparation and focusing and uneven sample lighting introduces an error in the results. Three areas from the each sample were measured. It was found that with the temperature varying from 560 to 610°C for the partial remelting, the volume fraction of liquid phase gradually increased in the semisolid microstructure with elevating of temperature. Fig.11 shows the curves of fraction liquid vs. temperature estimated by using an analytical solution based on Scheil equation compared with the curves estimated by DTA analysis and metallographic data for 7075 Al alloy with an extrusion ratio of 20. In

summary, it can be said that all three methods allow for a rough prediction of the phase fraction. This discussion shows clearly that, thermodynamic databases can be used to establish accurately the evolution of the liquid volume fraction during melting if the alloy is near equilibrium, or in conjunction with an appropriate model that account the thermal history of the alloy. Therefore, there is a need for experimental methods that evaluate directly the alloy on thermal conditions similar to the conditions employed by industrial practice. Nevertheless, the use of thermodynamic databases offers a very significant and unique advantage compared with all other methods. This method is a valuable tool for material selection and alloy design.

#### 4. CONCLUSIONS

In this study, the SIMA route has been shown to produce ideal, fine semi-solid microstructure, in which globular grains have a little amount of entrapped liquid. During partial remelting, liquid volume fraction, the average size and morphology of solid grains are influenced by the isothermal temperature and time. High semisolid isothermal temperature would reduce the solid volume fraction and accelerate the spherical evolution of the solid grains and led to coarsening of the grains. From line analysis it concluded that the contents of Cu at grain boundary increased, this means that the low melting structure at grain boundary was much influenced by Cu. As a result, weak mechanical properties of globular samples would appear if an alloy reheated at a high temperature. And the mechanical properties of samples after semisolid processing are weaker than the as-received materials and it due to the defects existing in globular samples. Thermodynamic simulation is a fast and efficient tool for the selection of alloys suitable for semi-solid processing.

#### REFERENCES

1. Jiang, H., Li., M., "Microscopic observation of cold-deformed Al–4Cu–Mg alloy samples after

- semi-solid heat treatments”, *Materials Characterization* 54 (2005) 451–457.
2. Fan, Z., “Semisolid metal processing”, *Int. Mater. Rev.* 47 (2002) 67.
  3. Atkinson, H. V., “Modeling the semisolid processing of metallic alloys”. *Progress in Materials Science* 50 (2005) 341–412.
  4. Chayong, S., Atkinson, H. V., Kapranos, P., “Thixoforming 7075 aluminum alloys”. *Materials Science and Engineering A* 390 (2005) 3–12.
  5. Dong, J., Cui, J. Z., Le, Q. C., Lu, G. M., “Liquidus semi-continuous casting, reheating and thixoforming of a wrought aluminum alloy 7075”. *Materials Science and Engineering A* 345 (2003) 234 – 242.
  6. Sang-Yong, L., Jung-Hwan, L., Young-Seon, L., “Characterization of Al 7075 alloys after cold working and heating in the semi-solid temperature range”. *Materials Processing and Technology* 111 (2001) 42±47.
  7. Zhang, L., Liu, Y. B., Cao, Z. Y., Zhang, Y. F., Zhang, Q. Q., “Effects of isothermal process parameters on the microstructure of semisolid AZ91D alloy”, produced by SIMA *Materials Processing and Technology* 209 (2009) 792-797.
  8. Saklakoglu, N., Saklakoglu, I., Tanoglu, M., Oztas, O., Cubukcuoglu, O., “Mechanical properties and microstructural evaluation of AA5013 aluminum alloy treated in the semi-solid state by SIMA process. *Mater.*”. *Process. Technol.* 148 (2004) 103–107.
  9. Shun-cheng, W., Yuan-yuan, L., Wei-ping, C., Xiao-ping, Z., “Microstructure evolution of semi-solid 2024 alloy during two-step reheating process”. *Trans Nonferrous Met Soc China* 18(2008) 784-788.
  10. Hong-min, G., Xiang-jie, Y., Meng, Z., “Microstructure characteristics and mechanical properties of rheoformed wrought aluminum alloy 2024”. *Trans Nonferrous Met Soc. China* 18 (2008) 555-561.
  11. Wang, J. G., Lin, H. Q., Wang, H. Y., Jiang, Q. C., “Effects of different processing parameters on the semisolid microstructure of the AZ91D alloy during partial remelting”. *Alloys and Compounds* 466 (2008) 98–105.
  12. Zhang, Q. Q., Cao, Z. Y., Zhang, Y. F., Su, G. H., Liu, Y. B., “Effects of compression ratio on the microstructure evolution of semisolid AZ91D alloy”. *Materials Processing Technology* 184 (2007) 195–200.
  13. ASTM E-8M. *Standard Test Methods for Tension Testing of Metallic Materials [Metric]*. ASTM international.
  14. Jufu, J., Ying, W., Jianjun, Q., Zhiming, D., Yi, S., Shoujing, L., “Microstructure evolution of AM60 magnesium alloy semisolid slurry prepared by new SIMA”. *Alloys and Compounds* 497 (2010) 62–67.
  15. Atkinson, H. V., Burke, K., Vaneetveld, G., “Recrystallisation in the semi-solid state in 7075 aluminum alloy”. *Materials Science and Engineering A* 490 (2008) 266–276.
  16. Kim, H. K., Kim, W. J., “Microstructural instability and strength of an AZ31 Mg alloy after severe plastic deformation”. *Materials Science and Engineering A* 385 (2004) 300–308.
  17. *Asm Handbook, Volume 3, Alloy Phase Diagrams*.
  18. Ming-bo, Y., Fu-sheng, P., Ren-ju, C., Jia, S., “Effects of holding temperature and time on semi-solid isothermal heat-treated microstructure of ZA84 magnesium alloy”. *Trans Nonferrous Met. Soc. China* 18 (2008) 566-572.